

A 400Gbit Ethernet core enabling High Data Rate Streaming from FPGAs to Servers and GPUs in Radio Astronomy

1 WEI LIU,¹ MITCHELL C. BURNETT,² DAN WERTHIMER,¹ AND JONATHON KOCZ¹

2 ¹*Department of Astronomy*
3 *University of California, Berkeley*
4 *425 Campbell Hall*
5 *Berkeley, CA, 94720-3411, USA*

6 ²*Department of Electrical And Computer Engineering*
7 *Brigham Young University*
8 *Provo, UT, 84602, USA*

ABSTRACT

10 The increased bandwidth coupled with the large numbers of antennas of several new radio telescope
11 arrays has resulted in an exponential increase in the amount of data that needs to be recorded and
12 processed. In many cases, it is necessary to process this data in real time, as the raw data volumes are
13 too high to be recorded and stored. Due to the ability of graphics processing units (GPUs) to process
14 data in parallel, GPUs are increasingly used for data-intensive tasks. In most radio astronomy digital
15 instrumentation (e.g. correlators for spectral imaging, beamforming, pulsar, fast radio burst and SETI
16 searching), the processing power of modern GPUs is limited by the input/output data rate, not by
17 the GPU's computation ability. Techniques for streaming ultra-high-rate data to GPUs, such as those
18 described in this paper, reduce the number of GPUs and servers needed, and make significant reductions
19 in the cost, power consumption, size, and complexity of GPU based radio astronomy backends.
20 In this research, we developed and tested several different techniques to stream data from network
21 interface cards (NICs) to GPUs. We also developed an open-source UDP/IPv4 400GbE wrapper for
22 the AMD/Xilinx IP demonstrating high-speed data stream transfer from a field programmable gate
23 array (FPGA) to GPU.

24 *Keywords:* Astronomical techniques, Astronomical instrumentation, Astronomy data acquisition

1. INTRODUCTION

25 Modern radio telescopes, such as the Square Kilometre Array (SKA)Schilizzi et al. (2007); Dewdney et al. (2009),
26 the Atacama Large Millimeter/submillimeter Array (ALMA)Brown et al. (2004), Deep Synoptic Array(DSA)Hallinan
27 et al. (2019); Connor et al. (2022) and MeerKATJonas & MeerKAT Team (2016) generate data at unprecedented
28 rates, reaching tens to hundreds of terabytes per second. This data needs to be transported from data acquisition
29 systems to real time processing units. There are different ways to process this data. Traditionally, an application
30 specific integrated circuit based system, such as the Wideband Interferometric Digital ARchitecture(WIDAR)Carlson
31 (2000) correlator, would be used. Alternatives include FPGA and more recently FPGA/GPU based hybrid systems.

32 In radio astronomy, it is typically desirable to process as much frequency bandwidth as possible. High-speed ADCs
33 are commonly used to process bandwidths of tens to hundreds of GHzJiang et al. (2020). To receive these data
34 streams, FPGAs with high-speed transceivers are utilized to receive, channelize and then subsequently transfer them
35 to data processing unitsAlvear et al. (2016); Liu et al. (2021). If these units are housed in a server (as is the case
36 for CPU or GPU based processing), this is typically done via one or more NICs. Between the NICs and the FPGAs,
37 high-speed Ethernet switch is also a critical part for the data transportation.

38 GPUs are renowned for their capacity for parallel processing, making them ideal for the computationally demanding
39 jobs needed for astronomical data analysis. For instance, Fast Fourier Transforms (FFTs) are utilized in GPUs to

43 transform time-domain signals into a frequency-domain representation Adámek et al. (2021). The performance of
 44 GPU-based FFTs is typically much better than CPU-based FFTs Ayala et al. (2022). Correlators need to receive and
 45 process data from several stations. The most common correlator implementation is known as the "FX correlator",
 46 which first channelizes the band using a polyphase filter bank, and then cross-multiplies each antennas channelized
 47 data with every other antenna's data. The computations can be done in parallel, which is ideal for GPUs Clark
 48 et al. (2013). In particular, Tensor-cores on the latest GPUs are special-purpose, matrix-matrix multiplication units
 49 that operate on limited-precision input data, which are good for correlator implementations Romein (2021). Various
 50 other common elements of a data processing pipeline for radio telescopes (such as an interference mitigation, calibration
 51 algorithms, and transient detection via beamforming and de-dispersion) can also be performed on GPUs Akeret et al.
 52 (2017); Agarwal et al. (2020); Yu et al. (2024).

53

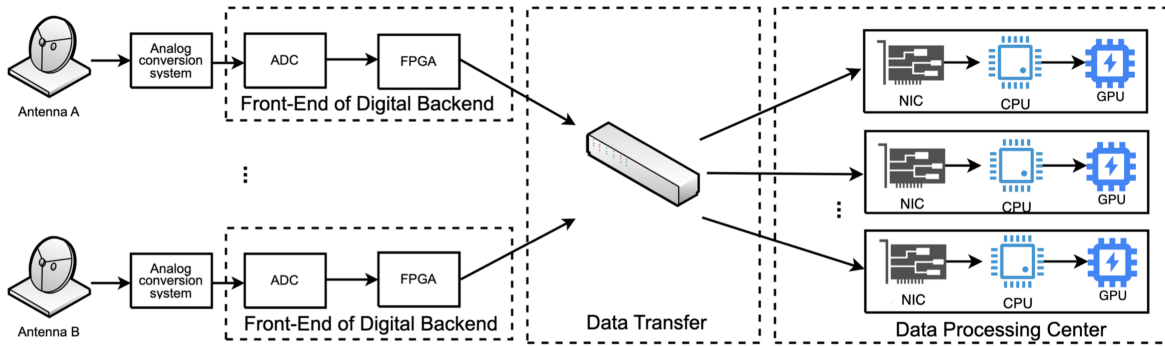


Figure 1. Diagram of a typical radio astronomy system showing the flow of data from telescopes to data processing centers. NICs, FPGAs, and GPUs are required to manage high-speed data streams.

54 Modern GPUs are powerful enough for most radio astronomy data processing applications. However, moving data
 55 between different system components, such as FPGAs to NICs to GPUs is often a limiting step in the data processing
 56 pipeline. Utilizing high-throughput interconnects such as Peripheral Component Interconnect Express (PCIe) and
 57 NVIDIA's "NVLink" Li et al. (2019) along with remote direct memory access (RDMA) technology Kalia et al. (2016)
 58 can mitigate these issues, however, it is still difficult to design, develop and implement a high-performance data
 59 transportation system. Additionally, while there are existing solutions (such as GPUDirect) for transferring large
 60 amounts of data between two GPU servers, the initial ingest (from e.g. an FPGA based system) is typically done via
 61 UDP packets, and is not necessarily able to take advantage of these techniques.

62 The Collaboration for Astronomy Signal Processing and Electronics Research (CASPER) aims to reduce this hurdle
 63 through the development of open source, general purpose hardware, libraries, tools, and reference instrument de-
 64 signs Hickish et al. (2016). These tools enable researchers to implement the high-performance instrumentation needed
 65 to achieve their science goals in a cost effective and timely manner.

66 The adoption of 400GbE in radio astronomy offers significant improvements in data transmission and processing
 67 capabilities. As radio telescopes collect vast amounts of data, the need for faster, more efficient data handling be-
 68 comes critical. 400GbE provides the necessary bandwidth to accommodate these large data rates, enabling real-time
 69 processing and analysis which are essential for timely discoveries and insights.

70 This paper outlines our research, beginning with the evaluation of RDMA techniques for bandwidth performance
 71 between NICs and GPUs. We then present the development of a 400GbE core with an FPGA for high-speed
 72 data transfer and an RDMA-based software framework for server-side data reception. This core will be integrated
 73 into the CASPER library, facilitating the rapid development of high-performance instrumentation by other researchers.

74

78 In Section 2, the core hardware components used for this research are listed, and estimates the capability of the
 79 hardware established; The RDMA techniques for transporting high-speed data streams from NICs to GPUs are demon-
 80 strated in Section 3, which includes moving data through the host memory (Section 3.2), and using GPUDirect tech-
 81 nology (Section 3.3, 3.4, 3.5); The implemented 400GbE core and associated test results for data transport from FPGA
 82 to NIC and then to GPUs are given in Section 4; A summary of all results and outlines for future research directions
 83 are provided in Section 5.

84 2. HARDWARE REQUIREMENTS FOR 400GBE

85 2.1. *System Description*

86 To transfer data from an FPGA to a GPU at 400 Gbps, it is important that all components in the data path are
 87 capable of operating at such speeds. This includes the FPGA, connecting cables, and all elements of the receiving
 88 server system. As RDMA is typically used to transfer high-speed data, RDMA technology should be supported by
 89 the NIC as well. A 400GbE NIC with a 16 lane PCIe 5.0 interface is required to support a theoretical maximum of
 90 512 Gb/s between the NIC and other devices (DRAM controller, CPU or GPUs) on the PCIe 5.0 bus. A PCIe 5.0
 91 motherboard and a PCIe 5.0 CPU are also necessary for the high data rate transportation. As DRAM is often used to
 92 transfer data to GPUs, having more DRAM controllers in the CPU will enhance performance. The NIC used for the
 93 tests described in this paper is the NVIDIA MCX75310AAS-NEAT¹, which supports PCIe 5.0 and 4x100 Gbps/lane;
 94 the CPU is Intel Xeon Silver 4410T², which contains 80 lanes of PCIe 5.0 and eight DDR5 controllers; the motherboard
 95 is a Gigabyte MS03-CE0³, which has seven PCIe 5.0 slots.

96 To test packet transfers from the FPGA, we need to be able to implement a 400GbE core on the FPGA board, which
 97 requires high-speed transceivers at a minimum. Because the NIC supports 100Gbps/lane, the FPGA transceivers
 98 should also support 100Gbps/lane. We choose the VPK180⁴ FPGA board based on AMD Versal Premium System on
 99 chip (SoC). Inside the Versal SoC, there are tens of GTM transceivers, which supports up to 112 Gbps when working
 100 in half-density mode.

102 The majority of GPUs currently on the market support up to PCIe 4.0, capable of transfers of at least 200 Gbps.
 103 Therefore, we used two PCIe 4.0 GPUs for these tests. GPUs can be broadly classified into two categories: gaming
 104 GPUs and scientific, or compute, GPUs. In Section 3 we compare the effectiveness of various data-moving techniques
 105 when comparing these two types of GPUs. The GPUs we tested are the NVIDIA RTX A6000⁵ and RTX 4070⁶.

108 Either copper cables or fiber optic links powered by transceivers are used for Ethernet interconnect. Inexpensive
 109 passive copper cables can be used for shorter distances (less than 3 meters for 400GbE), while fiber optic links, which
 110 can extend several kilometers, are needed for greater distances. In our work, we used copper cables from Fiberstore,
 111 which support the 400GBASE-CR4 interface standard. Table 1 summarizes the hardware used in this work.

113 2.2. *PCIe Bandwidth*

114 PCIe is a high-speed bus interface standard for connecting the peripheral hardware components of a computer
 115 system. It serves as the critical technology enabling communication between the motherboard and peripherals, such
 116 as GPUs and NICs. The achievable bandwidth for the different PCIe versions is shown in Table 2. The above rates
 117 are unidirectional. Full-duplex bidirectional rates are twice the table values.

118 As the PCIe bus is the primary mechanism for data transfer used by majority of devices, including the NICs and
 119 GPUs, it is important to measure the PCIe bus bandwidth in order to estimate the maximum performance that is
 120 achievable. Table 1 indicates that the system we built for testing has a bottleneck on GPUs, which have a PCIe 4.0
 121 interface, whereas other components support PCIe 5.0. To verify we achieve the PCIe 4.0 bandwidth, we used the

¹ <https://docs.nvidia.com/networking/display/connectx7vpi/specifications>

² <https://www.intel.com/content/www/us/en/products/sku/232388/intel-xeon-silver-4410t-processor-26-25m-cache-2-70-ghz/specifications.html>

³ <https://www.gigabyte.com/Enterprise/Server-Motherboard/MS03-CE0-rev-1x-3x>

⁴ <https://www.xilinx.com/products/boards-and-kits/vpk180.html>

⁵ <https://www.nvidia.com/en-us/design-visualization/rtx-a6000/>

⁶ <https://www.nvidia.com/en-us/geforce/graphics-cards/40-series/rtx-4070-family/>

Table 1. Core Hardware for 400GbE Evaluation

Hardware	Part Number	Specification
CPU	Intel Xeon Silver 4410T	80 lanes of PCIe 5.0; 8 memory channels of DDR 5
NIC	MCX75310AAS-NEAT	PCIe 5.0; 4 x 100Gbps/lane
Motherboard	MS03-CE0	7 x PCIe 5.0 slots; 8-Channel DDR5 slots
FPGA Board	VPK180	Transceivers support up to 112Gbps
GPUs	RTX A6000/ RTX 4070	PCIe 4.0 scientific/gaming GPUs
Copper cables	OSFP400-PC015	Support 400GBASE-CR4; OSFP-RHS cable for the NIC to NIC test
Copper cables	OSFPFL-400G-QDDPC01	Support 400GBASE-CR4; OSFP-RHS to QSFP-DD cable for the FPGA to NIC test

**Figure 2.** The server we setup for the 400G test, which includes 2 x RTX A6000(RTX 4070) GPUs, a 400G NIC, 8 x DDR5 DIMMs, a PCIe5.0 mother board and a PCIe5.0 CPU.

PCIe Version	Release Year	Transfer Rate (GT/s per lane)	Bandwidth (GB/s per lane)	Unidirectional Bandwidth (x16 configuration, GB/s)
1.0	2003	2.5	0.250	4.0
2.0	2007	5.0	0.500	8.0
3.0	2010	8.0	0.985	15.75
4.0	2017	16.0	1.969	31.5
5.0	2019	32.0	3.938	63.0
6.0	2022	64.0	7.877	126.0

Table 2. PCIe Versions and Their Associated Data Transfer Rates

code⁷ provided by NVIDIA to measure GPU bandwidth. The bandwidth performance for the RTX A6000 and RTX 4070 is shown in Figure 3(a) and Figure 3(b), respectively. Despite the substantial transfer rate achieved, this falls significantly short of the theoretical maximum transfer of 256 Gbps. The rates achieved do, however, match those

⁷ <https://github.com/liuweiseu/bandwidthtest/blob/master/bandwidthtest.cu>

126 achieved by NVIDIA with this code ⁸. As such, while it may be possible to achieve higher rates with, for example,
 127 other GPU models or drivers, we take this to be the limit of our current configuration for data capture and throughput
 128 testing purposes.
 129

<p>Device: NVIDIA RTX A6000 Transfer size (MB): 512</p> <p>Pageable transfers Host to Device bandwidth (GB/s): 8.726530 Device to Host bandwidth (GB/s): 19.170784</p> <p>Pinned transfers Host to Device bandwidth (GB/s): 24.979626 Device to Host bandwidth (GB/s): 26.353208</p>	<p>Device: NVIDIA GeForce RTX 4070 Transfer size (MB): 512</p> <p>Pageable transfers Host to Device bandwidth (GB/s): 8.172738 Device to Host bandwidth (GB/s): 15.021167</p> <p>Pinned transfers Host to Device bandwidth (GB/s): 25.108865 Device to Host bandwidth (GB/s): 26.303710</p>
<p>(a) RTX A6000 bandwidth performance</p>	<p>(b) RTX 4070 bandwidth performance</p>

Figure 3. Measured bandwidth performance of the RTX A6000 and RTX 4070 GPUs over a PCIe 4.0 interface. The results indicate a maximum achievable bandwidth of \sim 200 Gbps.

130

2.3. *Memory Bandwidth*

131 High-speed data transfer also depends on memory bandwidth, which in this case must have a minimum capacity
 132 of 400 Gbps in order to accommodate simultaneous 400 Gbps data streams. With eight DDR5 DIMMs operating
 133 at 4800 MHz and an eight DDR5 controller built into the CPU, the memory bandwidth is sufficient. The memory
 134 bandwidth is measured using the Intel Performance Counter Monitor (Intel PCM) tool⁹ and stress-ng^{10,11}, verifying
 135 that the 8-channel DDR5 memory bandwidth met the requirement for 400 Gbps data transfer (Figure 4).
 136

137

3. TECHNIQUES FOR DATA TRANSPORTATION FROM NIC TO GPU

138 Transmission Control Protocol/Internet Protocol (TCP/IP) and RDMA are crucial concepts for high-speed data
 139 transportation. Both techniques are used for data transfer, but they operate in fundamentally different ways and have
 140 distinct performance characteristics. This section discusses the differences between these approaches and showcases
 141 the performance of RDMA techniques using the test setup shown in Figure 5.
 142

143

3.1. *Remote Direct Memory Access*

144 TCP/IP, the fundamental set of communication protocols for the Internet and most local networks, consists of IP,
 145 TCP and UDP (User Datagram Protocol). Because of no buffering requirement, UDP is simpler to implement and
 146 allows for faster overall transmission speeds. In most radio astronomy applications, high-speed data transmission
 147 is unidirectional, from FPGAs to a data processing center, through a dedicated network. Consequently, UDP is
 148 commonly implemented.
 149

150

151 While it is simple to receive UDP streams using a Linux kernel UDP socket, it requires multiple buffer copies and
 152 heavy CPU usage, limiting its throughput. RDMA bypasses the host CPU and kernel, providing a high-throughput
 153 and low-latency network communication. Two outstanding features of RDMA are implemented in comparison to
 154 TCPIP: zero-copy and bypass kernel. The difference between UDP and RDMA is shown in Figure 6. For a 400GbE
 155 network, RDMA technology is essential for optimal performance.

⁸ <https://github.com/NVIDIA/nvbandwidth>

⁹ <https://github.com/intel/pcm>

¹⁰ <https://github.com/ColinIanKing/stress-ng>

¹¹ For best performance, please hand compile the benchmarks, since out of the box they wouldn't use the most efficient AVX.

```

|-----|-----|
|-- Socket 0
|-----|-----|
|-- Memory Channel Monitoring
|-----|-----|
|-- Mem Ch 0: Reads (MB/s): 8115.05 --|
|-- Writes(MB/s): 8098.09 --|
|-- PMM Reads(MB/s) : 0.00 --|
|-- PMM Writes(MB/s) : 0.00 --|
|-- Mem Ch 2: Reads (MB/s): 8115.27 --|
|-- Writes(MB/s): 8098.03 --|
|-- PMM Reads(MB/s) : 0.00 --|
|-- PMM Writes(MB/s) : 0.00 --|
|-- Mem Ch 3: Reads (MB/s): 8115.09 --|
|-- Writes(MB/s): 8098.06 --|
|-- PMM Reads(MB/s) : 0.00 --|
|-- PMM Writes(MB/s) : 0.00 --|
|-- Mem Ch 5: Reads (MB/s): 8115.20 --|
|-- Writes(MB/s): 8098.10 --|
|-- PMM Reads(MB/s) : 0.00 --|
|-- PMM Writes(MB/s) : 0.00 --|
|-- Mem Ch 6: Reads (MB/s): 8115.18 --|
|-- Writes(MB/s): 8098.13 --|
|-- PMM Reads(MB/s) : 0.00 --|
|-- PMM Writes(MB/s) : 0.00 --|
|-- Mem Ch 8: Reads (MB/s): 8115.93 --|
|-- Writes(MB/s): 8098.44 --|
|-- PMM Reads(MB/s) : 0.00 --|
|-- PMM Writes(MB/s) : 0.00 --|
|-- Mem Ch 9: Reads (MB/s): 8115.16 --|
|-- Writes(MB/s): 8098.07 --|
|-- PMM Reads(MB/s) : 0.00 --|
|-- PMM Writes(MB/s) : 0.00 --|
|-- Mem Ch 11: Reads (MB/s): 8116.04 --|
|-- Writes(MB/s): 8098.39 --|
|-- PMM Reads(MB/s) : 0.00 --|
|-- PMM Writes(MB/s) : 0.00 --|
|-- NODE 0 Mem Read (MB/s) : 64922.91 --|
|-- NODE 0 Mem Write(MB/s) : 64785.32 --|
|-- NODE 0 PMM Read (MB/s): 0.00 --|
|-- NODE 0 PMM Write(MB/s): 0.00 --|
|-- NODE 0 Memory (MB/s): 129708.23 --|
|-----|-----|
|-----|-----|
|-- System DRAM Read Throughput(MB/s): 64922.91 --|
|-- System DRAM Write Throughput(MB/s): 64785.32 --|
|-- System PMM Read Throughput(MB/s): 0.00 --|
|-- System PMM Write Throughput(MB/s): 0.00 --|
|-- System Read Throughput(MB/s): 64922.91 --|
|-- System Write Throughput(MB/s): 64785.32 --|
|-- System Memory Throughput(MB/s): 129708.23 --|
|-----|-----|

```

Figure 4. Memory bandwidth measurement of an 8-channel DDR5 memory configuration using the Intel Performance Counter Monitor (PCM) tool and stress-ng. The total memory bandwidth achieved is approximately ~ 1013 Gbps, meeting the requirements for 400 Gbps data transfer.

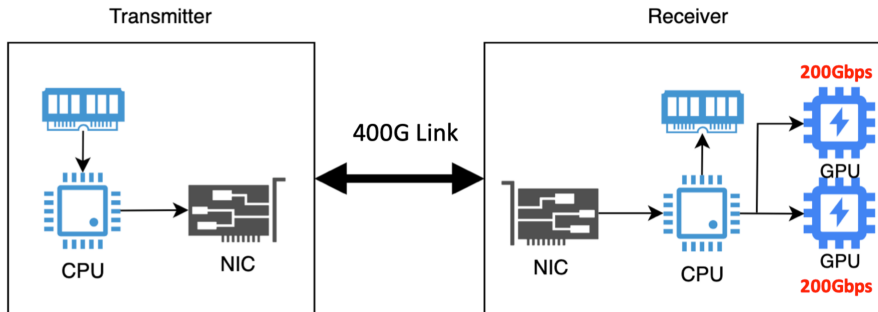


Figure 5. Setup of the 400G test servers used in the experiment. The servers are equipped with 400G NICs and GPUs to evaluate data transfer performance using various techniques.

156 Ibverbs (InfiniBand Verbs) is a low-level programming interface specifically made for InfiniBand/RDMA over
 157 Converged Ethernet(RoCE) networks that uses RDMA technology for high-performance network communication.
 158 Developers are able to design applications that demand exceptionally low latency and high throughput because to its
 159 direct access to the RDMA hardware. The OpenFabrics Enterprise Distribution (OFED) includes ibverbs as part of
 160 a broader suite of RDMA-supporting technologies.

161
 162 For the 400GbE core test, we select RDMA with ibverbs based on performance, compatibility, complexity, and
 163 system upgradeability. The 400GbE core generates UDP packets. On the receiver side, the Queue Pair type created

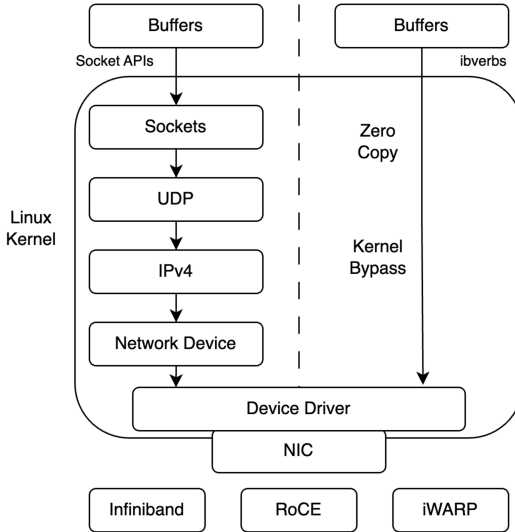


Figure 6. Comparison of data transfer processes using UDP and RDMA. The figure highlights the benefits of RDMA, including zero-copy and kernel bypass, which result in higher throughput and lower latency.

164 by ibverbs is RawEth, which captures UDP packets via kernel bypass and zero-copy.

165

166

3.2. NIC to DRAM to GPU

167 Data transfers from NIC to GPU via DRAM is a general method compatible with both gaming and scientific GPUs.
 168 For 400GbE applications, a full-duplex memory bandwidth of at least 800 Gbps is required. Our servers meet this
 169 memory bandwidth requirement, as shown in Section 2.3. Figure 7 illustrates the data transfer path from NIC to
 170 GPU through DRAM.
 171

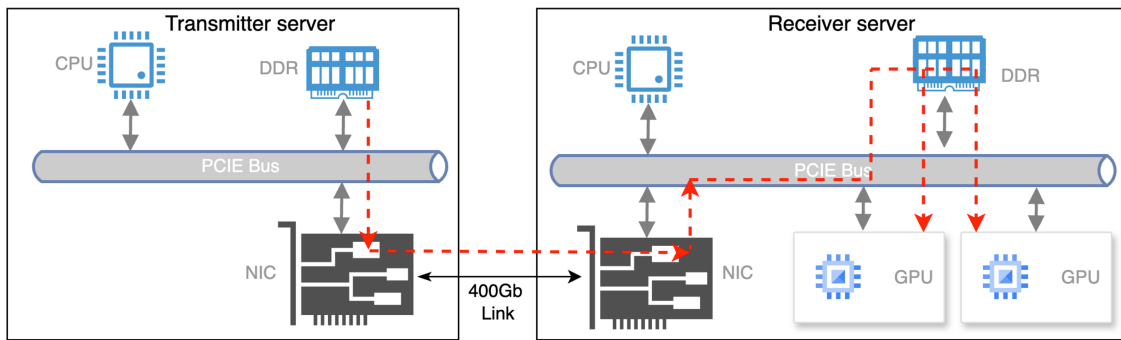


Figure 7. Data transfer path from NIC to GPUs via DRAM. This method utilizes the available memory bandwidth to handle high-speed data streams. Red dashed lines show the direction of data transfer.

172 In order to estimate the efficiency of data transfer from a NIC to GPUs via DRAM, a packet generator is developed
 173 on the transmitting server that sends packets using a 400GbE link. The maximum data rate of the packet generator
 174 is ~ 380 Gbps. As this exceeds the capture code capability, the speed of the generator is artificially limited to ensure
 175 we can the maximum data rate without packet loss. Each packet payload contains a packet sequence counter that
 176 was incremented by one. By examining the packet count sequence on the receiving end, we determine if there is any
 177 packet loss.
 178

179 The open Source HASHPIPE framework¹²¹³MacMahon et al. (2018) is used on the receiving server to capture
 180 packets and verify packet sequence values. Two threads, the network thread and gpu thread, are created in HASH-
 181 PIPE for receiving packets and moving packets to the GPUs. A shared memory buffer of status values is provided by
 182 HASHPIPE for real-time status monitoring. The HASHPIPE framework used in the test is shown in Figure 8.
 183

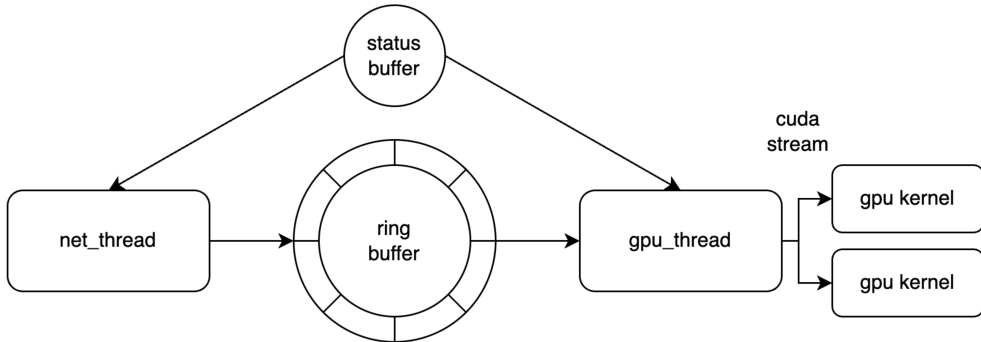
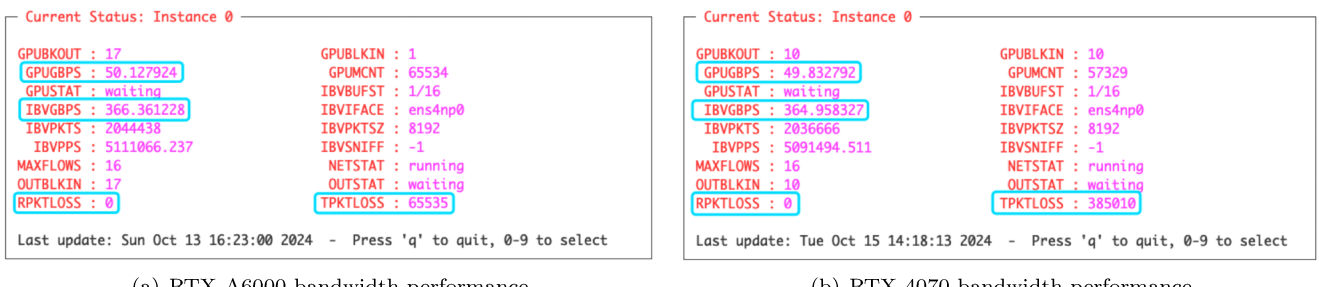


Figure 8. Architecture of the HASHPIPE framework used in the data transfer tests. The framework provides separate network and GPU threads for efficient packet handling, as well as provides real-time thread status monitoring.

184 The ibverbs APIs are used in the network thread and allow for receiving packets at a high data rate. Once the
 185 network thread receive packets from the 400G NIC, they transport the data to shared ring buffers in the host RAM.
 186 Data from the ring buffer were transferred to two GPUs using two CUDA streams in the gpu thread. To determine the
 187 data transfer rate, we measure the amount of time it takes to fill the ring buffer. Additionally, we verify the counter
 188 sequence values in received packets checking for packet loss. The calculated data rate and packet loss are stored in
 189 real time using the status buffer, shown in Figure 9(a)(RTX A6000) and Figure 9(b)(RTX 4070).
 190



(a) RTX A6000 bandwidth performance

(b) RTX 4070 bandwidth performance

Figure 9. Measured bandwidth performance of the RTX A6000 and RTX 4070 GPUs during the NIC to GPUs via DRAM test. Results show that the data transfer rate without packet loss is about 360 Gbps. RPKTLOSS shows the real-time packet loss, which is always zero after the initialization; TPKTLOSS shows the total number of packet loss, which is non-zero during the initialization, but remains constant after initialization.

3.3. Direct Data Transport from NIC to a Single GPU

191 GPUs and NICs, both PCIe devices, benefit from PCIe's high bandwidth and low latency when RDMA is used. In
 192 order to directly transfer data from NICs to GPUs, specific NICs and GPUs are needed: The NICs and GPUs should
 193 both be able to support RDMA. As we use NVIDIA NICs as well NVIDIA GPUs in this test, GPUDirect technology¹⁴
 194 can be used. GPUDirect allows GPUs to communicate directly with other system parts, bypassing the CPU and
 195 system memory, reducing latency and increasing throughput. Since both Tesla and Quadro GPUs support GPUDirect,
 196

¹² <https://github.com/david-macmahon/hashpipe>

¹³ <https://github.com/liuweiseu/hashpipe-ibverbs-demo.git>

¹⁴ <https://docs.nvidia.com/cuda/gpudirect-rdma/>

197 we utilized the RTX A6000 for the GPUDirect test. Figure10 shows the direct data transfer path from NIC to GPU
 198 using GPUDirect. As the PCIe limited IO bandwidth on the GPU is 200Gbps, we initially tested GPUDirect to one
 199 GPU with a 200G link.
 200

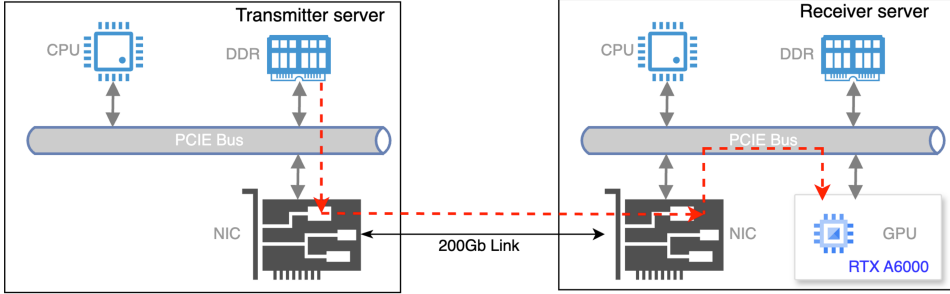


Figure 10. Direct data transfer path from NIC to GPU using GPUDirect technology. RDMA transactions reduces latency by bypassing the CPU and system memory. The link between the two servers is 200G. Red dashed lines shows the direction of data transfer.)

201 Packets on the transmitter server are generated using the ibverbs APIs and sent out in bursts to gauge bandwidth
 202 performance. Each burst transfers a total of 12.5 GB data, with each packet sizes to 8192 bytes and a total of
 203 1638400 packets. The receiving server also uses ibverbs to capture and report packet counts. The ibverbs routine
 204 (ibv_poll_cq¹⁵) reports how many packets are received successfully, so the packet loss can be checked by comparing
 205 the number of sent packets and the number of received packets. The RTX A6000 GPU supports PCIe 4.0, limiting
 206 throughput to 200Gbps. We achieved a maximum data rate of 178Gbps¹⁶ without packet loss, as shown in Figure11.
 207

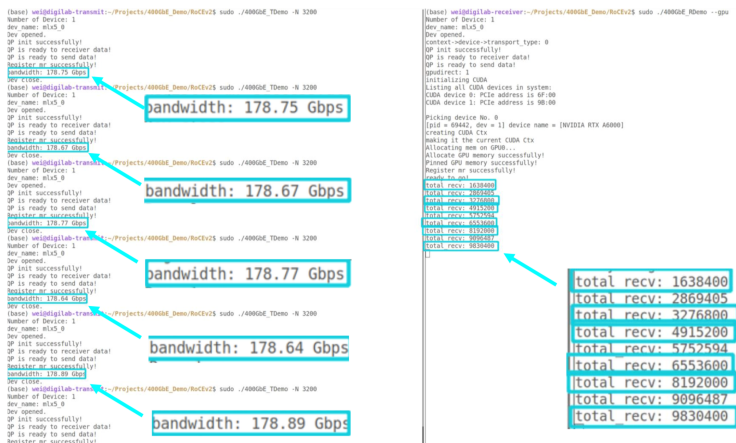


Figure 11. Measured bandwidth results of data transfers using GPUDirect to a single GPU on a 200 Gbps link. The maximum data rate achieved without packet loss is 178 Gbps. The packet loss is checked By comparing the number of sent packets and received packets. In each test, 1638400 packets are sent and 1638400 packets are received.

3.4. Direct data transport from NIC to two GPUs

209 As the 400G NIC is capable of supporting two 200Gbps links, and each GPU supports 200Gbps IO bandwidth, the
 210 capability of streaming to two GPUs simultaneously using GPUDirect was also tested. Figure 12 shows the direct
 211 data transfer path from NIC to two GPUs using GPUDirect.
 212

¹⁵ https://www.rdmamojo.com/2013/02/15/ibv_POLL_cq/

¹⁶ https://github.com/liuweiseu/400GbE_Demo.git

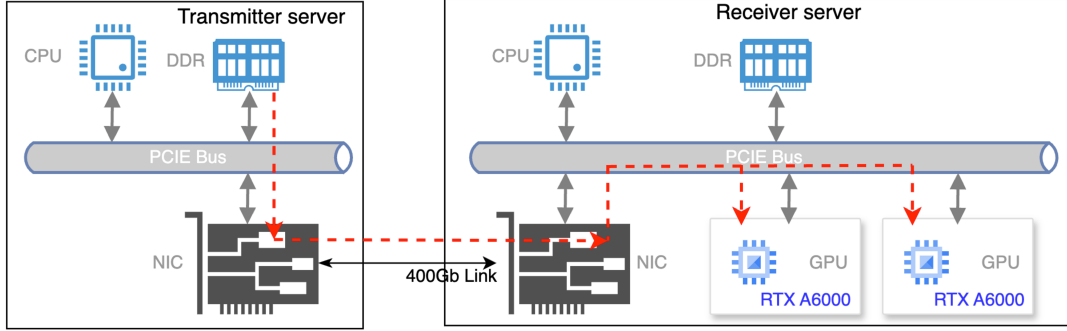


Figure 12. Direct data transfer path from NIC to two GPUs using GPUDirect technology. The link between the two servers is 400G link. Red dashed lines show the direction of data transfer.

213 On the transmitter server side, the same code based on ibverbs API mentioned in section 3.3 was used. In this case,
 214 however, the packets contain different source and destination port numbers. On the receiver server side, two receiving
 215 queue pairs with different flow are set for steering the two packet streams to the two GPUs. The resulting throughput
 216 (~180 Gbps) is shown in Figure 13.

```

Start to recv...
The number of ib devices is 1.
Open IB device successfully.
Create IB resources successfully.
Init IB resources successfully.
Allocate memory on GPU.
Allocate GPU memory successfully!
Pinned GPU memory successfully!
Register memory successfully.
Create flow successfully.
total_recv: 1111412 Bandwidth: 72.837 Gbps
total_recv: 2508005 Bandwidth: 91.527 Gbps
total_recv: 3904828 Bandwidth: 91.542 Gbps
total_recv: 5300936 Bandwidth: 91.495 Gbps
total_recv: 6698201 Bandwidth: 91.571 Gbps
total_recv: 8094774 Bandwidth: 91.526 Gbps
total_recv: 9490545 Bandwidth: 91.473 Gbps
total_recv: 10886989 Bandwidth: 91.517 Gbps
total_recv: 12283616 Bandwidth: 91.529 Gbps
total_recv: 13679394 Bandwidth: 91.474 Gbps
total_recv: 15074994 Bandwidth: 91.462 Gbps
  
```

GPUDirect to GPU0

```

Start to recv...
The number of ib devices is 1.
Open IB device successfully.
Create IB resources successfully.
Init IB resources successfully.
Allocate memory on GPU.
Allocate GPU memory successfully!
Pinned GPU memory successfully!
Register memory successfully.
Create flow successfully.
total_recv: 780366 Bandwidth: 51.142 Gbps
total_recv: 2176995 Bandwidth: 91.529 Gbps
total_recv: 3573712 Bandwidth: 91.535 Gbps
total_recv: 4969825 Bandwidth: 91.496 Gbps
total_recv: 6366914 Bandwidth: 91.560 Gbps
total_recv: 7763874 Bandwidth: 91.551 Gbps
total_recv: 9159603 Bandwidth: 91.470 Gbps
total_recv: 10555971 Bandwidth: 91.512 Gbps
total_recv: 11952608 Bandwidth: 91.530 Gbps
total_recv: 13348517 Bandwidth: 91.482 Gbps
total_recv: 14744203 Bandwidth: 91.468 Gbps
  
```

GPUDirect to GPU1

Figure 13. Measured bandwidth results of data transfers to two GPUs using GPUDirect on a 400Gbps link. The maximum data rate achieved is ~90Gbps \times 2.

218

3.5. Direct Data Transport from two NICs to two GPUs

219 While GPUDirect is based entirely on the PCIe bus similarly to RDMA, the performance was more limited, particularly when working with multiple GPUs. Besides measuring the performance of GPUDirect from one NIC to two GPUs, the performance of two pairs of NICs to GPUs with GPUDirect was also tested. The data transfer path is
220
221 shown in Figure 14, and the result (~ 276 Gbps) is shown in Figure 15. The improvement in this rate compared to
222 the single 400Gbps NIC suggests that the limitations in data rate transfer of the single NIC to two GPUs are due to
223 the GPUDirect configuration and PCIe lanes available in the case of a single NIC.
224

225

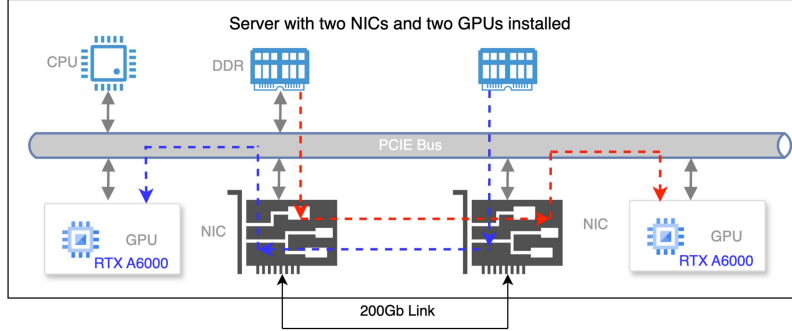


Figure 14. Direct data transfer path from two NIC to two GPUs on one server. Both of the two NICs send data to each other, and use GPUDirect to move the received data to two GPUs. The link is 200G. Red and blue dashed lines shows the direction of data transfer.

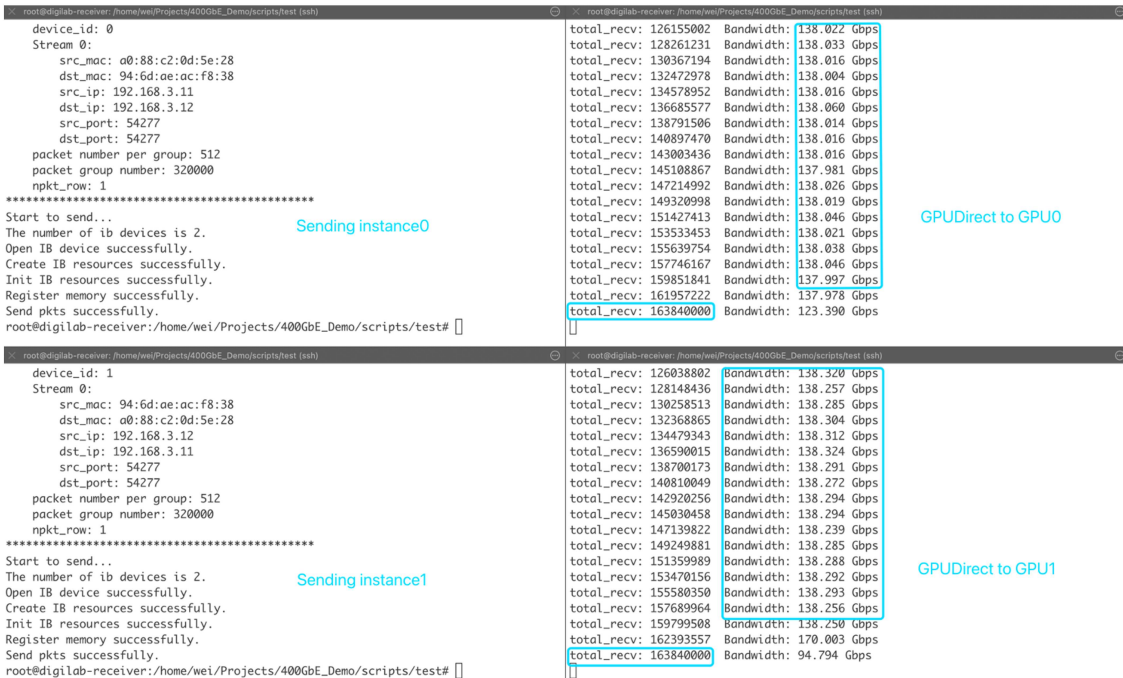


Figure 15. Measured bandwidth results of data transfers from two NICs to two GPUs using GPUDirect on a 200Gbps($\times 2$) link. The maximum data rate achieved is ~ 138 Gbps $\times 2$.

226

4. 400GbE FPGA CORE

The open source 400GbE FPGA core comprises two primary modules: the UDP packet generation core and the MAC/PHY core. The UDP packet generation core creates the UDP data packet and inserts the user-defined MAC address, IP address, port numbers into the packets. The MAC/PHY core, compliant with the IEEE 802.3ck-2022 400Gbps Ethernet standard, interfaces the FPGA with other devices over copper or optical transceiver modules. The AXI4 bus is used to transport control signals and statistical data. Figure 16 illustrates the core modules.

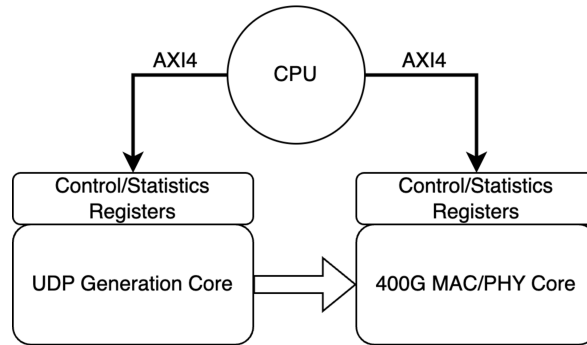


Figure 16. Block diagram of the 400GbE FPGA core shows the UDP packet generation and MAC/PHY core modules.

233

4.1. 400GbE Core Implementation

234

4.1.1. UDP packet generation core

The 400GbE UDP generation core, modified from the CASPER 100G core¹⁷, consists of two submodules: a streaming data module, and a CPU data module.

The streaming data module handles high-speed data transmission and reception to and from the 400G MAC/PHY core. It obtains MAC, IP, and port information via the AXI4 bus to produce packets at a high data rate, stored in registers or the ARP cache. For the TX data path, the module retrieves data from registers or an internal ARP cache, creates TX packets, and sends them to a TX ring buffer. For the RX data path, received packets are stored in an RX ring buffer and filtered by an RX filter to remove any unexpected packets with incorrect MAC, IP, or port numbers. The block diagram of the streaming data module is shown in Figure 17.

243

244

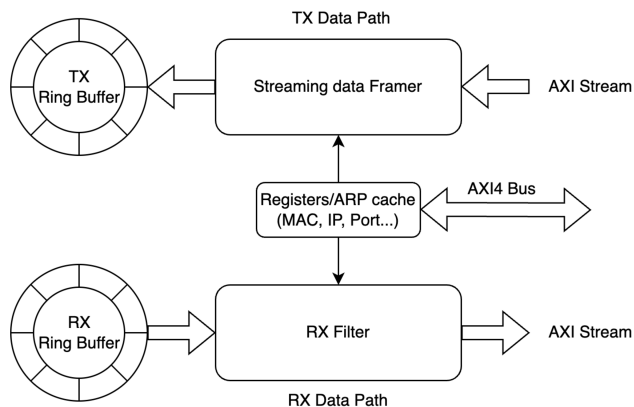


Figure 17. Block diagram of the streaming data module within the 400GbE FPGA core. The module handles high-speed data transmission and reception, including packet generation and filtering.

¹⁷ https://github.com/casper-astro/kutleng_skarab2_esp_firmware

245 The CPU data module sends and receives data to and from a microcontroller implemented in the FPGA. It shares
 246 registers, ARP cache, and the MAC/PHY core with the streaming module. An arbitration module determines which
 247 data to forward to the MAC/PHY core.

249 4.1.2. MAC/PHY Core

250 In the 400GbE FPGA core, the MAC/PHY core includes the Physical Coding Sublayer (PCS), Physical Medium
 251 Attachment (PMA), Physical Medium Dependent (PMD) layer, and support for varying numbers of lanes for various
 252 400GbE protocols.

253 We employ AMD's (Xilinx) GTM transceivers and 600G channelized multi-rate ethernet subsystem (DCMAC) core.
 254 The DCMAC is a high-performance, flexible, Ethernet-integrated hard IP that targets various networking applications.
 255 The 400GbE, 200GbE, and 100GbE combinations that the core supports allow for a maximum data rate of 600Gbps.
 256 For 400GbE, 200GbE, and 100GbE, it implements all of the 400G PCS operations, including: encoder, scrambler,
 257 alignment marker insertion, and forward error correction (FEC). Additionally, it partially performs the PMA function,
 258 freeing up 8 data lanes (two PCS lanes are consolidated into one) for GTM transceivers to connect to. For our open
 259 source 400GbE core design, the DCMAC core is a good choice because the hard IP on Versal SoC is supported by
 260 AMD with a free license.

262 With capabilities for up to 56Gbps per lane, the Versal SoC's GTM transceiver is the highest performing AMD
 263 transceiver. Working in full-density mode or half-density mode, it carries out the remaining PMA functions. For
 264 400GbE applications, the interface is 400GAUI-8 in full-density mode since each GTM transceiver operates indepen-
 265 dently; in half-density mode, two GTM transceivers cooperate to support 112Gbps per lane. In this scenario, the
 266 interface is 400GAUI-4. Since the NIC in our application supports 400GBASE-CR4, in order to obtain 106 Gbps/lane
 267 \times 4 lanes, we must configure the GTM in half density mode. We use two GTM quads to achieve the 400Gbps data
 268 throughput, because each GTM quad contains four GTM transceivers. The MAC/PHY core, based on DCMAC and
 269 GTM transceiver, is shown in Figure 18. The complete FPGA implementation of the 400GbE architecture is shown
 270 in Figure 19.

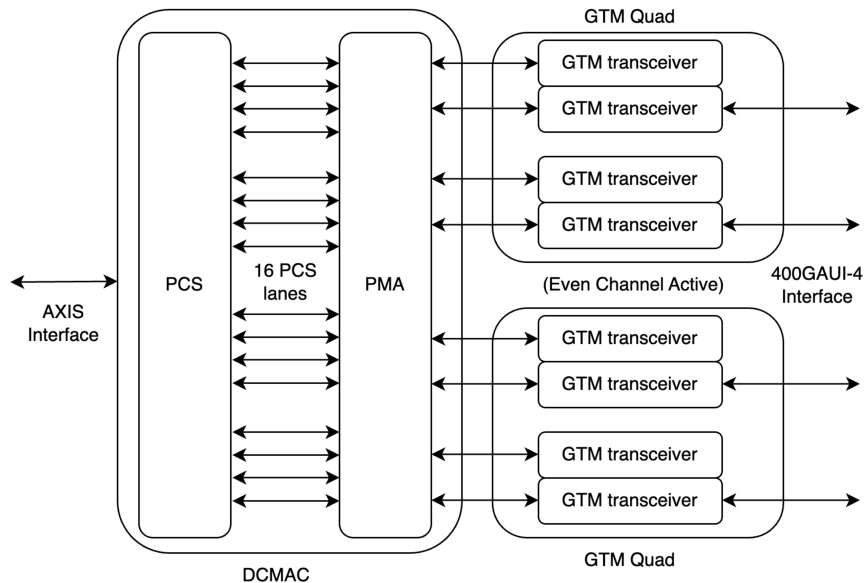


Figure 18. Integrated DCMAC core and GTM transceivers in the 400GbE MAC/PHY core. The components work together to support high-speed Ethernet communication.

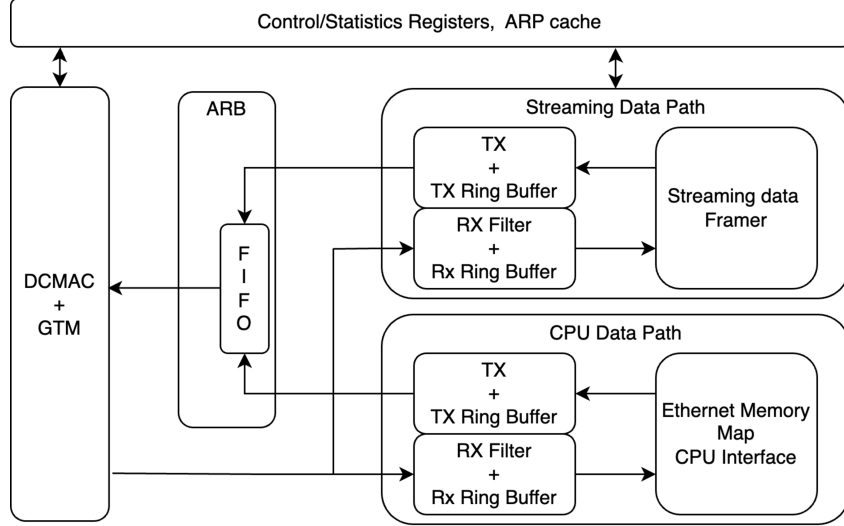


Figure 19. Complete architecture of the 400GbE FPGA core, illustrating the integration of various modules to achieve 400Gbps data transfer rates.

4.2. *FPGA to NIC to GPU through DRAM result*

To evaluate bandwidth performance of the 400GbE FPGA core, we developed a packet generation module that is connected to the 400GbE core. Each packet contains a 16-bit counter for packet loss detection, and the packet rate can be adjusted to obtain the data rate without packet loss. Using the same HASHPIPE framework-based code as described in Section 3.2, we monitor the packet loss status and real-time bandwidth measurement. Figure 20 illustrates the test setup, and Figure 21 shows the actual configuration.

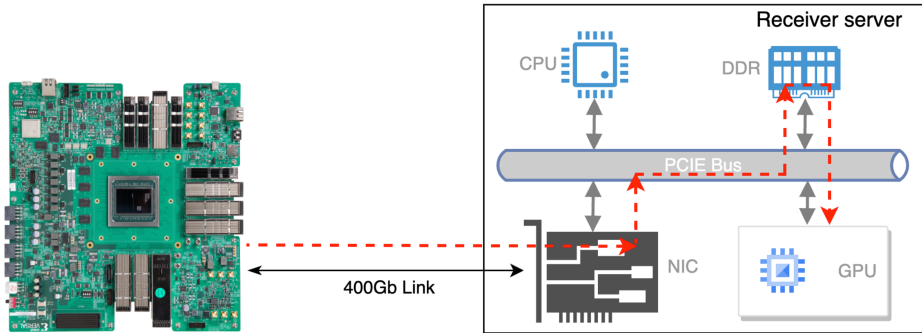


Figure 20. Diagram showing the setup for the FPGA to NIC to GPU via DRAM data transfer test. The setup includes the FPGA board, 400G NIC, and GPUs to evaluate data transfer performance.

Before further testing, we confirmed the 400G link between the FPGA and the server with a 400G NIC. Once configured with the 400GbE firmware, the server indicated an active state at 400G with four active lanes. Figure 22 shows the receiver NIC state.

The GPUs used in this test are two RTX A6000 and two RTX 4070. The clock rate on the FPGA side for generating packets and clocking the 400G Ethernet core is 390.625MHz, and the bus width of the DCMAC core is 1024 bits, so the total data rate from the DCMAC core is up to 400Gbps. After adjusting the speed of generating packets, the code running on the server side can capture the packets at up to \sim 362 Gbps without packet loss. We observed no packet loss with data rates up to 362 Gbps. This result is identical as we obtained in Section 3.2. Figure 23 shows the results of the FPGA to NIC to two GPUs test.

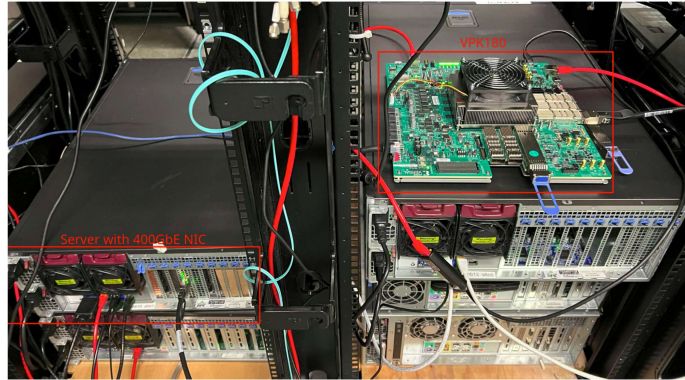


Figure 21. The actual setup used for the FPGA to NIC to GPU test. The setup demonstrates the hardware configuration and connections used in the experiment.

```
~$ sudo mlxlink -d mlx5_0 -e -c

Operational Info
-----
State : Active
Physical state : ETH_AN_FSM_ENABLE
Speed : 400G
Width : 4x
FEC : Standard_RS-FEC - (544,514)
Loopback Mode : No Loopback
Auto Negotiation : FORCE - 400G_4X

Supported Info
-----
Enabled Link Speed (Ext.) : 0x00010000 (400G_4X)
Supported Cable Speed (Ext.) : 0x00013ffe (400G_4X,200G_2X,200G_4X,100G_1
X,100G_2X,100G_4X,50G_1X,50G_2X,40G,25G,10G,5G,2.5G,1G)

Troubleshooting Info
-----
Status Opcode : 0
Group Opcode : N/A
Recommendation : No issue was observed

Tool Information
-----
Firmware Version : 28.40.1000
amBER Version : 2.8
MFT Version : mft 4.27.0-83
```

Figure 22. Status indication of the FPGA linked to the 400G NIC at a 400 Gbps data rate. The figure confirms the active state and link speed of the connection.

```
Current Status: Instance 0
-----
GPUBLKOUT : 23
GPUGBPS : 49.922611
GPUTSTAT : waiting
IBVGBPS : 363.305389
IBVPKTS : 2172371
IBVPPS : 5430898.540
MAXFLOWS : 16
OUTBLKIN : 23
RPKTLOSS : 0
GPUBLKIN : 7
GPUMCNT : 5472
IBVBUFST : 1/16
IBVIFACE : ens4np0
IBVPKTSZ : 8192
IBVSNIFF : -1
NETSTAT : running
OUTSTAT : waiting
TPKLOSS : 114693

Last update: Tue Oct 15 13:16:10 2024 - Press 'q' to quit, 0-9 to select
```

(a) RTX A6000 FPGA to GPU bandwidth performance

```
Current Status: Instance 0
-----
GPUBLKOUT : 20
GPUGBPS : 49.919478
GPUTSTAT : waiting
IBVGBPS : 363.306116
IBVPKTS : 2172379
IBVPPS : 5430909.416
MAXFLOWS : 16
OUTBLKIN : 20
RPKTLOSS : 0
GPUBLKIN : 4
GPUMCNT : 37179
IBVBUFST : 1/16
IBVIFACE : ens4np0
IBVPKTSZ : 8192
IBVSNIFF : -1
NETSTAT : running
OUTSTAT : waiting
TPKLOSS : 102716

Last update: Tue Oct 15 14:07:42 2024 - Press 'q' to quit, 0-9 to select
```

(b) RTX 4070 FPGA to GPU bandwidth performance

Figure 23. Test results of the FPGA to NIC to two GPUs data transfer, showing a data rate of 362Gbps without packet loss. RPKTLOSS shows the real-time packet loss, which is always zero after the initialization; TPKTLOSS shows the total number of packet loss, which is non-zero during the initialization, but remains constant after initialization. The figure illustrates the effectiveness of the 400GbE FPGA core in high-speed data transfer.

4.3. *FPGA to GPU Test Result with GPUDirect*

As the GPUs we are using in the tests have PCIe 4.0 interface with the speed limitation to \sim 200Gbps, what we expected is moving data into one GPU at \sim 200Gbps. To send packets from FPGA to two GPUs with GPUDirect technology, packets are sent out from FPGA with different source and dest port numbers, and these two kinds of packets are sent out one by one. On the server side, two queue pairs with different steer flows are created for directing the two kinds of packets into two GPUs. Figure 24 shows the test about FPGA to two GPUs with GPUDirect.

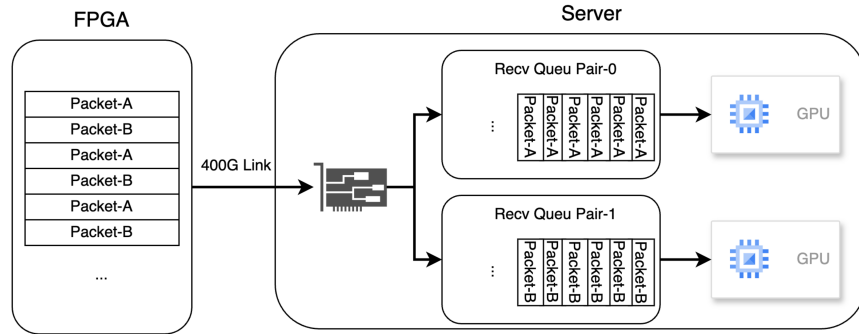


Figure 24. FPGA and server are connected with 400G link. FPGA sends out two kinds of packets with different source and dest port numbers: Packet-A and Packet-B. The data stream are steered to two queue pairs with different steer flow, and then sent to two GPUs directly.

If only one receiving queue pair is enabled, half of the data will be sent to one GPU. The bandwidth is about ~ 180 Gbps, which is identical to the result mentioned in section 3.3; If both of the two receiving queue pairs are enable, the one data stream will be split to two data streams, and the data will be sent to two GPUs at the same time directly. The bandwidth of each data stream is ~ 90 Gbps, and the total bandwidth is ~ 180 Gbps. The results about this test are shown in Figure 25(a) and figure25(b).

```
Allocating memory on GPU.
Allocate GPU memory successfully!
Pinned GPU memory successfully!
Register memory successfully.
Create flow successfully.
total_recv: 530154 Bandwidth: 34.744 Gbps
total_recv: 3057615 Bandwidth: 165.639 Gbps
total_recv: 5584760 Bandwidth: 165.616 Gbps
total_recv: 8111901 Bandwidth: 165.619 Gbps
total_recv: 10871648 Bandwidth: 180.862 Gbps
total_recv: 13647187 Bandwidth: 181.897 Gbps
total_recv: 16422726 Bandwidth: 181.897 Gbps
total_recv: 19198224 Bandwidth: 181.895 Gbps
total_recv: 21973792 Bandwidth: 181.899 Gbps
total_recv: 24749349 Bandwidth: 181.898 Gbps
total_recv: 27524851 Bandwidth: 181.895 Gbps
total_recv: 30300400 Bandwidth: 181.898 Gbps
[]

x root@digilab-receiver:~/home/we/Projects/400GbE_Demo/scripts/Recv (ssh)
dst_ip: 192.168.3.12
src_port: 54278
dst_port: 54278
use_gpu: 1, gpu_id: 1
nsge: 1
disable_recv: 1
*****
Start to recv...
The number of ib devices is 3.
Open IB device successfully.
Create IB resources successfully.
Init IB resources successfully.
Allocate memory on GPU.
Allocate GPU memory successfully!
Pinned GPU memory successfully!
Register memory successfully.
Create flow successfully.
total_recv: 814971 Bandwidth: 53.410 Gbps
total_recv: 2211083 Bandwidth: 91.496 Gbps
total_recv: 3607634 Bandwidth: 91.524 Gbps
total_recv: 5004839 Bandwidth: 91.515 Gbps
total_recv: 6400649 Bandwidth: 91.528 Gbps
total_recv: 7796209 Bandwidth: 91.459 Gbps
total_recv: 9192310 Bandwidth: 91.495 Gbps
total_recv: 10588388 Bandwidth: 91.493 Gbps
[]

x root@digilab-receiver:~/home/we/Projects/400GbE_Demo/scripts/Recv (ssh)
Open IB device successfully.
Create IB resources successfully.
Init IB resources successfully.
Allocate memory on GPU.
Allocate GPU memory successfully!
Pinned GPU memory successfully!
Register memory successfully.
Create flow successfully.
total_recv: 131553 Bandwidth: 8.621 Gbps
total_recv: 1527580 Bandwidth: 91.490 Gbps
total_recv: 2924165 Bandwidth: 91.527 Gbps
total_recv: 4320544 Bandwidth: 91.513 Gbps
total_recv: 5716966 Bandwidth: 91.516 Gbps
total_recv: 7113164 Bandwidth: 91.501 Gbps
total_recv: 8508744 Bandwidth: 91.461 Gbps
total_recv: 9905153 Bandwidth: 91.515 Gbps
total_recv: 11300900 Bandwidth: 91.472 Gbps
[]
```

(a) GPUDirect from FPGA to GPU with one queue pair enabled (b) GPUDirect from FPGA to GPU with two queue pairs enabled

Figure 25. GPUDirect from FPGA to NIC results. If one queue pair is enabled on the receiver side, the bandwidth is about ~ 180 Gbps; if both of the two queue pairs are enabled, bandwidth for each data stream is ~ 90 Gbps, and total is about ~ 180 Gbps.

301 5. SUMMARY AND FUTURE WORK

302 This study examines the bandwidth performance of two RDMA techniques: moving data through DRAM and
 303 GPUDirect, when transferring data from NIC to GPUs. Moving data to GPUs through DRAM can achieve approxi-
 304 mately 180 Gbps to a single GPU without packet loss and about 360 Gbps to two GPUs. With GPUDirect, we can
 305 transfer \sim 180Gbps to a single GPU, and \sim 90Gbps \times 2 to two GPUs simultaneously. Using two NICs and two GPUs
 306 with GPUDirect can achieve the bandwidth of \sim 138Gbps \times 2. When using GPUDirect to two GPUs from a single
 307 NIC, the data rate was half of that expected. In the case of the dual NICs to dual GPUs the data rate improved,
 308 but was still below that achieved when transferring the data via DRAM. We plan to conduct research on further
 309 high-performance computing methods in the future, including Data Plane Development Kit (DPDK) and Holoscan in
 310 order to compare the performance of these approaches to our current results.

312 In addition to the server to server tests, a 400GbE FPGA core was developed. As many radio telescopes using a
 313 networked architecture, this allowed the testing of a typical radio astronomy scenario where simple UDP packets were
 314 transmitted to a server. Using this core, data rates of 362 Gbps were transferred without experiencing any packet
 315 loss between the FPGA and two GPUs. Testing with GPUDirect, the 400GbE FPGA core can transfer data at about
 316 180 Gbps to one GPU. This core will be added to the CASPER library, and the test results demonstrate the potential
 317 of RDMA techniques and the FPGA 400GbE core for high data rate applications.

319 6. ACKNOWLEDGEMENT

320 The authors would like to thank John Romein (ASTRON) for his advice on 400G NIC settings, Andre Renard
 321 (UofT) for his advice on memory bandwidth improvement, Adam Thompson and Cliff Burdick (NVIDIA) for their
 322 assistance with the NIC to NIC tests, and Leo Karnan (AMD) for his advice on GTM transceiver settings. The authors
 323 also thank to AMD's University Program for their donation of the VPK180 FGPA board. The research was funded
 324 by NSF grants 2009537 and 2307781.

510 REFERENCES

511 325 Adámek, K., Novotný, J., Thiyagalingam, J., & Armour,
 326 W. 2021, IEEE Access, 9, 18167

512 327 Agarwal, D., Lorimer, D., Surnis, M., et al. 2020, Monthly
 328 Notices of the Royal Astronomical Society, 497, 352

513 329 Akeret, J., Chang, C., Lucchi, A., & Refregier, A. 2017,
 330 Astronomy and computing, 18, 35

514 331 Alvear, A., Finger, R., Fuentes, R., et al. 2016, in
 332 Millimeter, Submillimeter, and Far-Infrared Detectors
 333 and Instrumentation for Astronomy VIII, Vol. 9914,
 334 SPIE, 332–345

515 335 Ayala, A., Tomov, S., Luszczek, P., et al. 2022, Univ.
 336 Tennessee at Knoxville, Knoxville, TN, USA, Tech. Rep.
 337 ICL-UT-22-02

516 338 Brown, R. L., Wild, W., & Cunningham, C. 2004,
 339 Advances in Space Research, 34, 555

517 340 Carlson, B. 2000, Implementation, and Signal Processing,
 341 NRC-EVLA Memo, 1

518 342 Clark, M. A., Plante, P. L., & Greenhill, L. J. 2013, The
 343 International journal of high performance computing
 344 applications, 27, 178

519 345 Connor, L., Bouman, K. L., Ravi, V., & Hallinan, G. 2022,
 346 Monthly Notices of the Royal Astronomical Society, 514,
 347 2614

520 348 Dewdney, P. E., Hall, P. J., Schilizzi, R. T., & Lazio, T.
 349 J. L. 2009, Proceedings of the IEEE, 97, 1482

521 350 Hallinan, G., Ravi, V., Weinreb, S., et al. 2019, arXiv
 351 preprint arXiv:1907.07648

522 352 Hickish, J., Abdurashidova, Z., Ali, Z., et al. 2016, Journal
 353 of Astronomical Instrumentation, 5, 1641001

523 354 Jiang, H., Yu, C.-Y., Chen, M., & Liu, M. 2020,
 355 Publications of the Astronomical Society of the Pacific,
 356 132, 085001

524 357 Jonas, J., & MeerKAT Team. 2016, in MeerKAT Science:
 358 On the Pathway to the SKA, 1, doi: [10.22323/1.277.0001](https://doi.org/10.22323/1.277.0001)

525 359 Kalia, A., Kaminsky, M., & Andersen, D. G. 2016, in 2016
 360 USENIX Annual Technical Conference (USENIX ATC
 361 16), 437–450

526 362 Li, A., Song, S. L., Chen, J., et al. 2019, IEEE Transactions
 363 on Parallel and Distributed Systems, 31, 94

527 364 Liu, W., Meng, Q., Wang, C., et al. 2021, Journal of
 365 Instrumentation, 16, P08047

528 366 MacMahon, D. H., Price, D. C., Lebofsky, M., et al. 2018,
 367 Publications of the Astronomical Society of the Pacific,
 368 130, 044502

529 369 Romein, J. W. 2021, Astronomy & Astrophysics, 656, A52

370 Schilizzi, R., Alexander, P., Cordes, J., et al. 2007, SKA
371 Memorandum, 100

372 Yu, Z., Deng, F., Sun, S., et al. 2024, Research in
373 Astronomy and Astrophysics